

Origins of Structural Hole Traps in Hydrogenated Amorphous Silicon

Eric Johlin,^{1,*} Lucas K. Wagner,² Tonio Buonassisi,¹ and Jeffrey C. Grossman^{1,†}

¹Massachusetts Institute of Technology, Cambridge, Massachusetts 02139, USA

²University of Illinois, Urbana, Illinois 61801, USA

(Received 2 August 2012; revised manuscript received 14 November 2012; published 5 April 2013)

The inherently disordered nature of hydrogenated amorphous silicon (*a*-Si:H) obscures the influence of atomic features on the trapping of holes. To address this, we have created a set of over two thousand *ab initio* structures of *a*-Si:H and explored the influence of geometric factors on the occurrence of deep hole traps using density-functional theory. Statistical analysis of the relative contribution of various structures to the trap distribution shows that floating bonds and ionization-induced displacements correlate most strongly with hole traps in our ensemble.

DOI: [10.1103/PhysRevLett.110.146805](https://doi.org/10.1103/PhysRevLett.110.146805)

PACS numbers: 73.50.Gr, 61.43.Dq, 73.61.Jc, 73.61.-r

Over the last four decades, much work has been done toward understanding both the origins of the low efficiency of hydrogenated amorphous silicon (*a*-Si:H) solar cells, and how the properties limiting efficiency can be improved. Two main factors have been attributed to this low overall efficiency—the Staebler-Wronski effect (SWE) [1], (a performance degradation under exposure to light; normally leading to a $\sim 10\%$ current drop in optimized cells [2]), and the inherent low hole mobility in the material (typically around 5 orders of magnitude lower than crystalline silicon) [2,3], although the causes of both of these properties are still not fully understood. This uncertainty is rooted in the inherently disordered nature of amorphous materials, which severely complicates theoretical analysis. For our purposes here, we focus on the defects contributing to the initial low mobility, although there is substantial evidence that by improving this property, the degradation from the SWE can be curtailed as well [4–6].

Extended discussions concerning the nature of the defects limiting the hole mobility of the material have appeared in the literature over the past decades. Early works asserted that the major defect was the dangling bond (threefold, under-coordinated Si atoms), controlling both the deep, midgap states directly [7–9], as well as the shallower bandtail states (often through secondary mechanisms, e.g., conversion between dangling and weak bonds) [8,10–13]. Floating bonds [fivefold overcoordinated Si atoms; see Fig. 1(a)] were also implicated [14–18], although this alternate theory never seemed to gain as much traction. The view of midgap states controlling the initial mobility has since declined, with both computational and experimental works providing evidence that the bandtails control the mobility of holes, and that these states are expressed independent of midgap state concentrations [19,20]. This has been accompanied by an evolution of alternate theories on the sources of these bandtail states, indicting other structural phenomena, such as strained bonds or filaments [21–24], movement of hydrogen [25–28], and incorporation of mono- and divacancies in the material

nanostructure [29], as correlated to the trapping of holes in the material. Despite this plethora of investigations, there has been little consensus as to the nature of the bandtail traps, which, we believe, is exacerbated by a lack of studies on the statistics of causal relationships between atomic structure and hole trapping.

In this Letter, we address this uncertainty through three main contributions: first, we create and validate a large ensemble of *ab initio* hydrogenated amorphous silicon structures, providing what we believe is an accurate computational model of the bulk material. Second, through the application of statistics to density-functional theory-determined properties of our ensemble, we explore the relative contributions of wide-ranging structural defects to hole trapping distributions, allowing us to concomitantly clarify the prevalence and severity of these defects in our ensemble. Finally, using this data, we are able to provide insight into a possible trap state in which reversible silicon atom displacements allow holes to self-trap in highly stable (deep trap) configurations [Fig. 1(b)], with a stronger

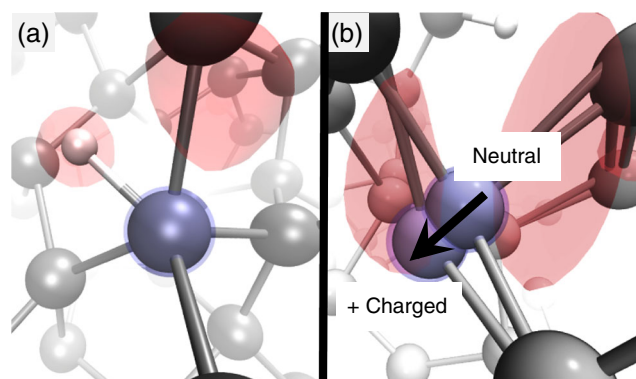


FIG. 1 (color online). Hole 50% probability location density (red) for (a) floating bond defect, and (b) reversible atomic displacement causing hole self-trapping. The central defect atoms are in blue, and show hole wave function localization near said defects.

correlation to substantial trap states than any other examined defect.

Computer modeling of amorphous materials has two conflicting needs: on the one hand, accurate treatment of electrons is required, and on the other, to accurately reproduce the bulk disordered system, large samples of atomic configuration space are necessary. Calculating a large set of geometries and taking the ensemble as a whole for the purpose of analysis allows us to approximate the diversity of configurations present in a bulk layer, while balancing between the prohibitive computational expense of inordinately large structures, and the inaccuracies of few, small geometries. To this end, our work is performed on a set of 2700 virtual samples (split into 1200 sample *training* and 1500 sample *test* subsets) of 216 Si and 20 H atoms, with the size chosen to minimize computational expense, while reducing finite size errors due to the (charged) periodic system and the amorphous network. An approximate 10% hydrogen atomic concentration was chosen to fit with the nominal concentration set in experimental materials optimized for PV performance [30]. For details on the sample creation, see the Supplemental Material [31].

Previous studies have mostly examined the energy level of the highest occupied molecular orbital (HOMO) as a metric for the hole trap depth of a structure. While this approach does indeed give the positive-charge ionization energy of the initial geometry, it also presents potential problems: first, the accuracy of this energy level for reasonable time scales cannot be assured, as substantial atomic relaxation could occur during the presence of the hole in the localized area, especially in regions with already relatively low ionization energy. Furthermore, beyond the introduction of uncertainty into the distribution of ionization potentials, simply using the HOMO level to infer the hole trap depth ignores the possibility of self-trapped holes.

For these reasons, the *a*-Si:H geometries in our ensemble are re-run from the neutral configuration with one electron removed (a net +1 eV charge applied), and again allowed to fully relax within density-functional theory (DFT). This provides us with the positive charge energy of the sample (E_+). We use this in combination with the neutral charge configuration energy (E_0) to compute the adiabatic ionization potential, $I_n = E_0 - E_+$, of the structure—a measure of how energetically expensive it is for a hole to be present in a given structure in our virtual bulk amorphous silicon material. These calculations were repeated on a random subset of structures using the higher-accuracy HSE06 hybrid functional, confirming excellent agreement with the original PBE energy trends. An energy shift was noted, but as all comparisons made rely on relative energies, this does not affect our following results (see Supplemental Material [31]).

Once the ionization potential has been determined for all 2700 samples, we select a reference energy, I_0 , from which to base the calculation of each samples' hole trap depth $\text{HTD}_n = I_n - I_0$. It is necessary to take the hole trap depth as a relative quantity, as it is the energy change between

any given sample and the set as a whole that determines the difficulty of a hole moving from one location in a material to the next. We select the mode ionization potential as the reference energy of our ensemble so that the movements within the bulk of the distribution will correspond to a hole trap depth of ~ 0 eV. The comparison of the fully relaxed ensemble to that of simply using the unrelaxed energy (or HOMO energy level of the neutral sample) is illustrated in Fig. 2.

To ensure self-consistency in this method, the sample geometries must be fully reversible between the uncharged and charged states, as an irreversible relaxation caused by the removal of an electron would be expressed as a large energy difference, but would not indicate a case of strong hole trapping. This reversibility is verified through re-neutralizing the charged geometry, allowing it to relax fully again, and comparing this third structure with that of the original neutral sample. In the fairly rare cases in which changes are present, the re-neutralized sample is then set as the base configuration, and the process repeated until the neutral energies converge. All samples were found reversible between the neutral and charged states after at most two of the above-described steps. It is interesting to note that the process of hole addition causing a favorable relaxation could actually be capturing some real physical occurrence (as electric biasing of *a*-Si:H does show cell efficiency improvements and works to reverse some SWE degradations [32]; and the introduction of an electron to a hole trap location has been previously offered as an explanation for the SWE [3]), but for the scope of this study the phenomena was simply used as a limit on the phase space

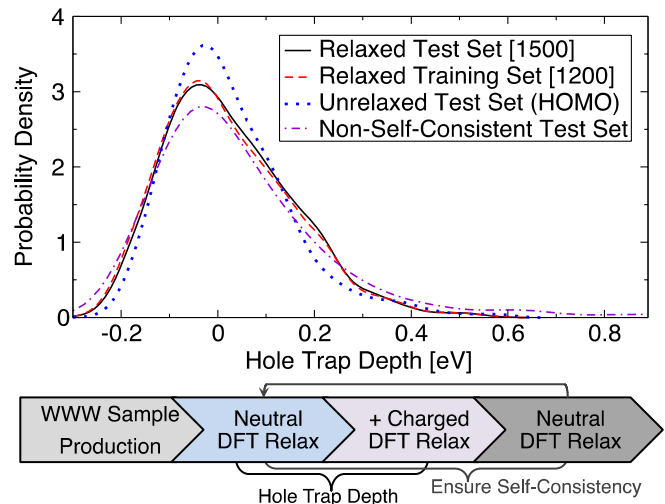


FIG. 2 (color online). Comparison of the test set (used to verify and display trends) to the training set (used to determine trends), as well as to the test set before the positive charge relaxation (misses many trap structures; appears overly ideal), and the test set before the application of the self-consistency requirement (includes some absolute relaxations; includes unphysical hole traps). The flow diagram below depicts the sample creation process.

of our set to ensure self-consistent hole trap depth measurements. The flow of this process, as well as a comparison to the non-self-consistent ensemble, is also depicted in Fig. 2.

For our samples, we have verified agreement with experiment between various structural parameters, such as bulk density [33], the radial pair distribution function [34,35], bulk modulus [30], and qualitative structural occurrences (such as the unassisted appearance of hydrogenated nanovoids in some structures), as shown in the Supplemental Material [31]. Furthermore, the additional total energy of the structures produced for this study above the corresponding crystalline geometry match results obtained via recent differential scanning calorimetry experiments [36,37] remarkably well (0.07–0.15 eV/atom experimental; 0.07–0.17 eV/atom in our calculations).

Having established and vetted a computational set of α -Si:H structures, we are able to explore causation between geometric features and hole trapping as follows: by calculating a hole trap depth distribution of our full ensemble (using kernel density estimation [38,39]), we can compare this to conditional distributions with samples expressing certain features removed. If the conditional distribution does not contain hole trap states, then we can say that either the removed defect causes hole trap states, or there is a common cause between it and the trap states.

While the potential selections for these conditions are enormous, and many tested (average or extrema bond lengths and angles, density, etc.) criteria showed no statistically relevant relationships, we present three here that we believe demonstrate interesting characteristics of our set. For “improvement,” we are most strongly considering a decrease in the positive hole trap depths, although narrowing of the distribution in general is beneficial, with the limiting case (a perfect crystal) being a Dirac delta function. It is also important to note that the number of samples present in the conditional set determines the resolution of the distribution, and so for each conditional ensemble we list the number of samples meeting the applied criteria in brackets after the sample label in the legend of the plot.

We begin by investigating the oft-asserted culprits behind the deepest hole traps: dangling and floating bonds. In order to define dangling and floating bonds, we inspect the local environment of each silicon atom in each structure, noting the 4th- and 5th-closest atomic distances: a short 5th-closest distance indicates a floating bond, while a long 4th-closest distance indicates a dangling bond. Through the examination of the probability distribution of overcoordinated Si atoms (short 5th-closest distance in a structure) and undercoordinated Si atoms (long 4th-closest distance) in Fig. 3(a), we are able to define what we consider bonding: we take the minimum of the 5th bond distribution at 2.75 Å as the cutoff criterion. Analyzing this distribution and its role on the hole traps in our ensemble, we observe several interesting phenomena. First, the prevalence of floating bonds exceeds those of dangling bonds in our ensemble, supporting the views of Pantelides [17], that floating bonds are the more-abundant coordination defect in α -Si:H. Second, we see that the

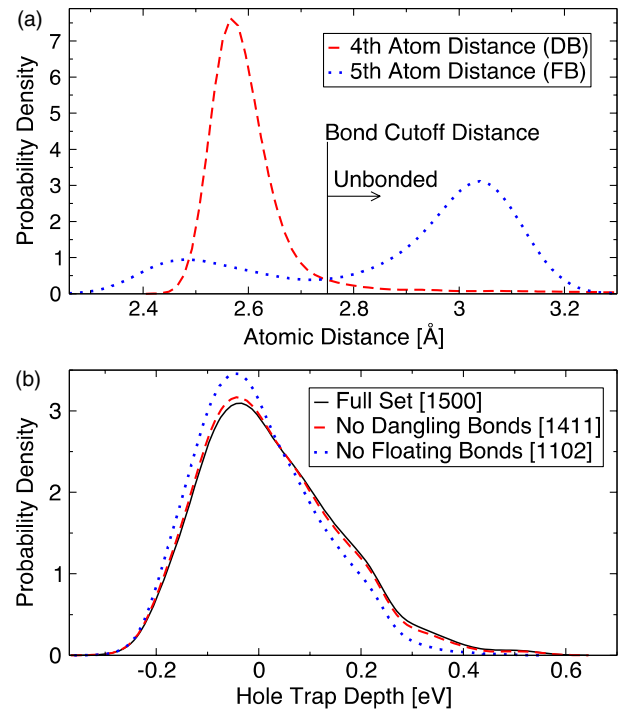


FIG. 3 (color online). (a) Distributions of the longest 4th and shortest 5th atomic distances prevalent in each sample (see text). (b) Hole trap depth distributions displaying relative strength of dangling bond and floating bond coordination defects.

floating bond is substantially more defined, although both defects are indeed continuously present from distances of ~ 2.5 to 3.2 Å. Examining the conditional probability distribution of the ensemble [Fig. 3(b)], we observe that the removal of floating bond-containing samples idealizes the distribution substantially more than the removal of dangling bond-containing samples. This indicates that floating bonds are not only more prevalent in our ensemble, but correlate more strongly to hole traps as well. Finally, we notice that while the removal of all floating and dangling bond samples from our ensemble does improve the distribution (most notably around $+0.2$ eV), there still remains a substantial density of hole trap structures that are unexplained by these coordination defects.

To understand these remaining hole traps, we next examine the maximum silicon atom displacement in our samples under hole introduction (referred to from here as “displacement” for succinctness). As seen in Fig. 1(b), substantial displacement can occur during charge introduction into a sample. This is important for three reasons: first, the hole preferentially localizes near the displacing atom, indicating that the displacement is allowing the hole to self-trap in the reconfigured structure. Second, the displacement is entirely reversible—by limiting our sample phase space to structures with repeatable hole trap depths under relaxation we ensure (and have manually verified) that the displacement observed is indeed a metastable defect promoting hole self-trapping and not simply a lowering of the total energy of the system. Finally, the displacement is accompanied by

substantial hole trap depths: as seen in Fig. 4(a), by applying an increasingly strict “maximum allowed displacement” criterion to the conditional probability distributions of hole traps in our ensemble, we observe increasingly idealized distributions, indicating that the prevalence of reversible atomic displacement is strongly correlated with hole trap depth. Furthermore, comparing the conditional distribution excluding structures featuring high displacements to that in which we exclude coordination defects [Fig. 4(b)], we observe that the influence of self-trapped holes linked to atomic movement outweighs even those of the dangling and floating bonds combined. The confluence of all these conditions together, however, improves the distribution even further, indicating that these features are indeed distinct, and complementary in their influence on hole trapping. The trends mentioned above (correlations between hole trap depths and floating bonds or combined coordination defects, and ionization displacements) were confirmed using a Kolmogorov-Smirnov test to be statistically relevant (unique from their parent distribution) to over 95% confidences (see Supplemental Material [31] for details).

Last, we examine the correlation between the hole trap depth of the structure and the localization length of the hole wave function in the charged state. The localization length is computed via the methods presented by Resta and Sorella [40], and Silvestrelli [41]. As seen in Fig. 5, we observe a strong bias toward negative trap depths (hole barriers) in the samples with the longest hole localization lengths, whereas the structures with localized holes (short lengths) express higher trap depths. While the correlation is quite strong at

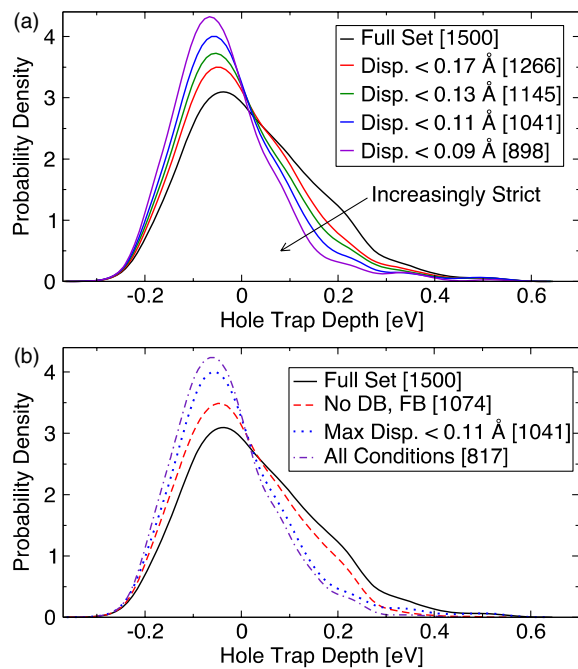


FIG. 4 (color online). Hole trap depth distributions (a) displaying the effect of an increasingly strict “maximum displacement” criterion continually excluding reversible displacement defects, and (b) compared to coordination defects, and the congregation of all listed defects.

the shortest localization lengths, as the length increases the correlation to stronger traps appears to initially increase, peak, and then reduce, suggesting a balance between two opposing forces: structural phenomena energetically favoring the hole to localize nearby, balanced against the kinetic energy driving the hole to delocalize. This lends credence to the ionization displacement effect, in that it motivates the view that the displacements are occurring to allow a relative delocalization of the hole in its confined state to mitigate this “overconfinement” energy penalty.

The major contributions of this work can be summarized as follows: First, the demonstration that ionization-induced atomic displacement expresses the strongest causal relationship to hole trapping of any of the investigated structural features. This bolsters the view that *a*-Si:H is indeed a fluctuating material, in contrast to the static geometry of its crystalline counterpart. Second, we provide evidence for the exoneration of dangling bonds as the major coordination defect in the material, and instead implicate floating bonds as the more significant contribution to limiting hole mobility. Finally, we provide further evidence as to the importance of moderate delocalization of the hole wave function in producing deep trap states. While these results do challenge some previous theories, many of the more recent contributions are in no way mutually exclusive, and some well supported by these findings—for example, the recent work by Drabold [23,24], correlating the presence of the tail electron states proximate to static bond-distorted “filaments,” fits well with our observations that the highest trap states are correlated with higher levels of delocalization.

The results presented here provide insight into potential methods of preventing these traps, and thereby improving the material electronic transport properties. For example, recent advances in the understanding of stress [42–44] could be used in leveraging strain in samples to prevent atomic displacements, as could attempts at targeted annealing to crystallize or reamorphize regions under which metastable displacement defects are present. While these correlations advance the understanding of the nature of

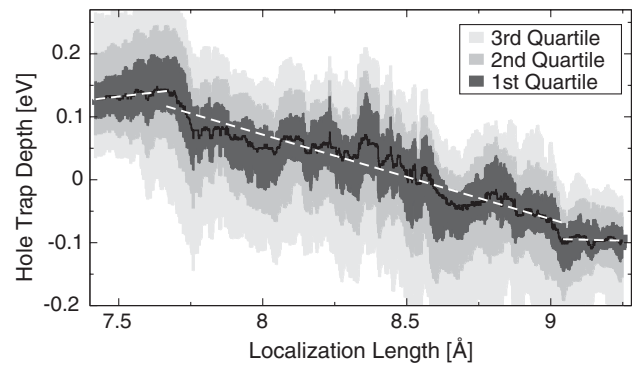


FIG. 5. Correlation showing peak hole trap depth at an intermediate hole wave function localization length. The gray solid areas represent quartiles in the trap depth probability distributions, with the black line indicating the center of the distribution, and the dashed white line a piecewise linear regression to the data.

structural hole-trapping defects in hydrogenated amorphous silicon, we hope that more knowledge can be gleaned from the created ensemble of geometries. To this end, the entire set of 2700 *a*-Si:H structures will be made freely available online (via the Supplemental Material [31]), with the hope that a readily available large ensemble of amorphous silicon geometries will foster further discoveries based on statistical analysis of the set. Finally, we hope that beyond the specific system of *a*-Si:H, both the statistical methods utilized here, as well as the results supporting the importance of self-trapping defects could prove useful in the study of any disordered systems concerned with bandtail states (for example, disordered organics and polymers).

We acknowledge and thank C. B. Simmons (MIT), E. P. Stephen (Boston University), and D. A. Strubbe (MIT) for helpful discussions. The authors would like to thank the King Fahd University of Petroleum and Minerals in Dhahran, Saudi Arabia, for funding the research reported in this Letter through the Center for Clean Water and Clean Energy at MIT and KFUPM under Project No. R1-CE-08. The authors also acknowledge the Texas Advanced Computing Center (TACC) at The University of Texas at Austin for providing HPC resources that have contributed to the research results reported within this Letter.

*johlin@alum.mit.edu

†jcg@mit.edu

- [1] D. L. Staebler and C. R. Wronski, *Appl. Phys. Lett.* **31**, 292 (1977).
- [2] R. A. Street, *Hydrogenated Amorphous Silicon* (Cambridge University Press, Cambridge, England, 1991).
- [3] E. A. Schiff, *J. Non-Cryst. Solids* **352**, 1087 (2006).
- [4] J. Shirafuji, M. Kuwagaki, T. Sato, and Y. Inuishi, *Jpn. J. Appl. Phys.* **23**, 1278 (1984).
- [5] J. Shirafuji, K. Shirakawa, and S. Nagata, *Jpn. J. Appl. Phys.* **25**, L634 (1986).
- [6] H. Fritzsche, *Annu. Rev. Mater. Res.* **31**, 47 (2001).
- [7] D. K. Biegelsen and M. Stutzmann, *Phys. Rev. B* **33**, 3006 (1986).
- [8] M. Stutzmann and D. K. Biegelsen, *Phys. Rev. B* **40**, 9834 (1989).
- [9] M. Stutzmann and D. K. Biegelsen, *Phys. Rev. Lett.* **60**, 1682 (1988).
- [10] Y. Bar-Yam and J. D. Joannopoulos, *Phys. Rev. Lett.* **56**, 2203 (1986).
- [11] R. A. Street, J. Kakalios, and T. M. Hayes, *Phys. Rev. B* **34**, 3030 (1986).
- [12] Z. E. Smith and S. Wagner, *Phys. Rev. Lett.* **59**, 688 (1987).
- [13] H. M. Branz and E. A. Schiff, *Phys. Rev. B* **48**, 8667 (1993).
- [14] S. T. Pantelides, *J. Non-Cryst. Solids* **97–98**, 79 (1987).
- [15] J. H. Stathis and S. T. Pantelides, *Phys. Rev. B* **37**, 6579 (1988).
- [16] S. T. Pantelides, *Phys. Rev. Lett.* **60**, 1683 (1988).
- [17] S. T. Pantelides, *Phys. Rev. Lett.* **57**, 2979 (1986).
- [18] J. H. Stathis, *Phys. Rev. B* **40**, 1232 (1989).
- [19] J. Liang, E. A. Schiff, S. Guha, B. Yan, and J. Yang, *Appl. Phys. Lett.* **88**, 063512 (2006).
- [20] Q. Wang, H. Antoniadis, and E. A. Schiff, *Appl. Phys. Lett.* **60**, 2791 (1992).
- [21] P. A. Khomyakov, W. Andreoni, N. D. Afify, and A. Curioni, *Phys. Rev. Lett.* **107**, 255502 (2011).
- [22] L. K. Wagner and J. C. Grossman, *Phys. Rev. Lett.* **101**, 265501 (2008).
- [23] Y. Pan, F. Inam, M. Zhang, and D. A. Drabold, *Phys. Rev. Lett.* **100**, 206403 (2008).
- [24] D. A. Drabold, Y. Li, B. Cai, and M. Zhang, *Phys. Rev. B* **83**, 045201 (2011).
- [25] R. Biswas, Q. Li, Y. Yoon, and H. M. Branz, *Phys. Rev. B* **56**, 9197 (1997).
- [26] H. M. Branz, *Phys. Rev. B* **59**, 5498 (1999).
- [27] H. M. Branz, *Phys. Rev. B* **60**, 7725 (1999).
- [28] S. Zafar and E. A. Schiff, *Phys. Rev. Lett.* **66**, 1493 (1991).
- [29] J. Melskens, A. H. M. Smets, M. Schouten, S. W. H. Eijt, H. Schut, and M. Zeman, *2012 38th IEEE Photovoltaic Specialists Conference* (IEEE, Bellingham, WA, 2012).
- [30] A. H. Mahan, J. Carapella, B. P. Nelson, R. S. Crandall, and I. Balberg, *J. Appl. Phys.* **69**, 6728 (1991).
- [31] See Supplemental Material at <http://link.aps.org/supplemental/10.1103/PhysRevLett.110.146805> for details of the structure creation and vetting process used for the ensemble formation, as well as elaboration on the methods used.
- [32] D. E. Carlson and K. Rajan, *Appl. Phys. Lett.* **70**, 2168 (1997).
- [33] H. Ohsaki and Y. Tatsumi, in *Properties of Amorphous Silicon and Its Alloys*, edited by T. Searle (Institution of Engineering and Technology, London, 1998), p. 347.
- [34] K. Laaziri, S. Kycia, S. Roorda, M. Chicoine, J. L. Robertson, J. Wang, and S. C. Moss, *Phys. Rev. Lett.* **82**, 3460 (1999).
- [35] R. Bellissent, A. Menelle, W. S. Howells, A. C. Wright, T. M. Brunier, R. N. Sinclair, and F. Jansen, *Physica (Amsterdam)* **157B**, 217 (1989).
- [36] F. Kail, J. Farjas, P. Roura, C. Secouard, O. Nos, J. Bertomeu, and P. R. I. Cabarrocas, *Phys. Status Solidi* **5**, 361 (2011).
- [37] D. A. Drabold, *Phys. Status Solidi* **5**, 359 (2011).
- [38] M. Rosenblatt, *Ann. Math. Stat.* **27**, 832 (1956).
- [39] E. Parzen, *Ann. Math. Stat.* **33**, 1065 (1962).
- [40] R. Resta and S. Sorella, *Phys. Rev. Lett.* **82**, 370 (1999).
- [41] P. L. Silvestrelli, *Phys. Rev. B* **59**, 9703 (1999).
- [42] E. Johlin, N. Tabet, S. Castro-Galnares, A. Abdallah, M. I. Bertonni, T. Asafa, J. C. Grossman, S. Said, and T. Buonassisi, *Phys. Rev. B* **85**, 075202 (2012).
- [43] H. Gleskova and S. Wagner, *J. Non-Cryst. Solids* **354**, 2627 (2008).
- [44] H. Gleskova, P. Hsu, Z. Xi, J. Sturm, Z. Suo, and S. Wagner, *J. Non-Cryst. Solids* **338–340**, 732 (2004).